Separation Science and Technology
Publication details, including instructions for authors and subscription information:
http://www.informaworld.com/smpp/title~content=t713708471

Studies on the In Situ Electrooxidation and Selective Permeation of Cerium(IV) across a Bulk Liquid Membrane Containing Tributyl Phosphate as the Ion Transporter

C. S. Kedari[a]; S. S. Pandit[a]; A. Ramanujam[a]
[a] FUEL REPROCESSING DIVISION, BHABHA ATOMIC RESEARCH CENTRE, TROMBAY, MUMBAI, INDIA

To cite this Article Kedari, C. S. , Pandit, S. S. and Ramanujam, A.(1999) 'Studies on the In Situ Electrooxidation and Selective Permeation of Cerium(IV) across a Bulk Liquid Membrane Containing Tributyl Phosphate as the Ion Transporter', Separation Science and Technology, 34: 9, 1907 — 1923
To link to this Article: DOI: 10.1081/SS-100100746
URL: http://dx.doi.org/10.1081/SS-100100746

SEPARATION SCIENCE AND TECHNOLOGY, **34**(9), pp. 1907–1923, 1999

Studies on the In Situ Electrooxidation and Selective Permeation of Cerium(IV) across a Bulk Liquid Membrane Containing Tributyl Phosphate as the Ion Transporter

---

C. S. KEDARI, S. S. PANDIT, and A. RAMANUJAM*
FUEL REPROCESSING DIVISION
BHABHA ATOMIC RESEARCH CENTRE
TROMBAY, MUMBAI-400 085, INDIA

ABSTRACT

The results of experiments carried out to develop a liquid membrane (LM) technique for the extractive permeation of cerium from nitric acid solutions are described. In-situ electrooxidation of Ce^{3+} to extractable Ce^{4+} and its transport across bulk LM (BLM) composed of tri-*n*-butyl phosphate (TBP)/dodecane mixtures was systematically studied under varied hydrodynamical and chemical conditions. The permeability of metal ions across the BLM was dependent on the efficiency of extraction, ionic activity of feed solutions, stirring rate, composition of the receiving phase, etc. The transport rates were found to vary linearly (a log–log correlation) with the cation concentration in feed solutions and concentration of TBP in BLM. A permeation velocity equation for cerium ion through the membrane has been proposed. More than 90% permeation of Ce with a maximum flux of 8.63×10^{-5} mol/m^2/s could be accomplished under the experimental conditions: stirring rates at feed and strip solutions were 380 and 300 rpm, respectively; feed was 1 mol·dm^{-3} of HNO_3 containing 0.005 mol·dm^{-3} $Ce(NO_3)_3$; LM contained 30% TBP/dodecane; and the receiving phase was distilled water. Radiochemically pure Ce-144 was partitioned from the Ce–Am mixture obtained by extraction chromatographic fractioning of high level radioactive waste. This also resulted in the purification of Am-241 in the feed solution with a decontamination factor of ~12 from Ce.

Key Words. Cerium(IV); Tributyl phosphate; Dodecane; Liquid membrane; Permeation; Electrooxidation; Purex process

---

* To whom correspondence should be addressed.

www.dekker.com

INTRODUCTION

Current emphasis on the production and purification of lanthanides and transplutonium elements brings greater demands on separation chemists. Recovery of radioactive lanthanides from Purex process high level radioactive active waste solutions has a dual benefit. First, there is a large demand in various fields for lanthanides recovered in their purest form (1, 2). Second, the radiotoxicity of radioactive effluents is reduced during partitioning and transmutation of actinides (3). The partitioning and transmutation process requires partitioning of transplutonium elements from Purex high level waste (HLW) solutions with minimum concentration of neutron poisoning impurities for the subsequent transmutation process (4, 5). The intra- and intergroup separations of lanthanides and trivalent actinides are most difficult to achieve (6–9). Extensive work has been carried out in our laboratory on the fractionation of HLW with extraction chromatography techniques using octyl(phenyl)-*N*,*N*-diisobutylcarbamoylmethylphosphine oxide (CMPO) and an indigenously synthesized solvent, 2-ethylhexyl, 2-ethylhexyl phosphonic acid (KSM-17, equivalent to PC 88A) as extractants (10, 11). These methods exploit small differences in the solution chemistry of lanthanide-actinide elements. The above processes are not effective for individual separation of Ce–Am because of their very close ionic radii and charge densities. An imposed variation of valency state of transition elements is of great use in hydrometallurgical separation of these cations. We recently reported an in-situ electrooxidation and liquid–liquid extraction of Ce^{4+} into dodecane with tributyl phosphate (TBP) and KSM-17 extractants (12). In-situ electrooxidation gives greater yield compared to chemical oxidation and also avoids the introduction of additional impurities into the process solution.

Compared with liquid–liquid extraction based on the partition principle between two phases (aqueous and organic), the extraction of metal ions by a liquid membrane (LM) is based on their transportation by means of permeation through an LM. An LM is a liquid phase which separates two other liquid phases with which it is immiscible. For example, in the liquid membrane system depicted in Fig. 1, metal ions are transported from one water phase (the source phase, SP) to the other water phase (the receiving phase, RP) through the membrane. As a technique it has number of advantages such as low energy consumption, possibility of using expensive but highly specifics extractant molecules, high separation factor, upgrading the concentration of the recovered species, etc. (13–16). To achieve the required selectivity, the dynamic (chemical and transport) characteristics of process (i.e., diffusion of metal species from the SP to the SP–LM interface, reaction of metal species with the carrier molecule at the SP–LM interface, diffusion of the metal–carrier

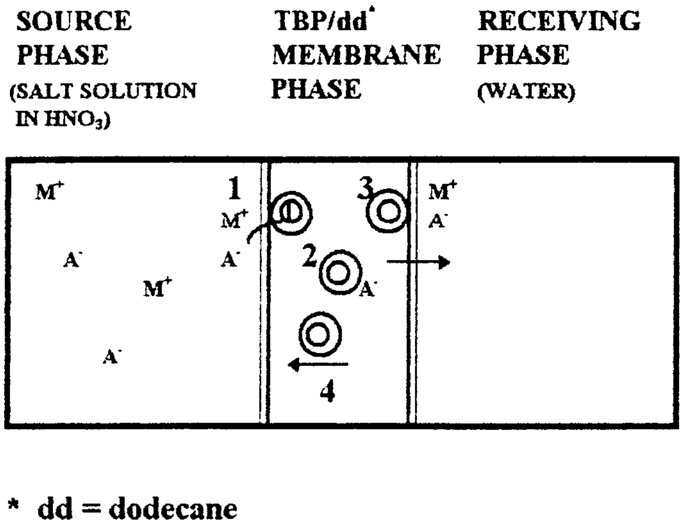

FIG. 1 Transport of Ce salt across liquid membrane. (1) Cation M^+ in the source phase moves into the membrane phase (accompanied by anion A^-) and is complexed by TBP (represented by circle). (2) Complex–anion pair moves across the membrane. (3) Cation and anion are released to the receiving phase. (4) Ligand returns to repeat the cycle.

complex through the LM phase, release of metal ions into the RP at the RP–LM interface and diffusion of metal species into the RP) play an important role (17). The principle of such a separation technique was explained by Danesi (18). The LM has been studied under different geometrical configurations, such as bulk liquid (BLM), supported liquid (SLM), emulsion liquid (ELM) membranes, etc. (19). Recently Vijayakumar et al. (20) described a system composed of integrated baffle plates cell with an efficiency as high as that of ELM and the simplicity of a BLM. In the present investigation, a single baffle plate LM cell compatible to the given separation has been used.

Optimization studies have been carried out for the development of an LM technique to separate and recover Ce from nitric acid solutions, employing TBP/dodecane as a metal transporter in the LM phase. TBP is the most popular extractant in actinide purifications (21) and also acts as a carrier in various membrane processes (22, 23). The most useful property of this reagent is its fast extraction and easy stripping of metal ions from the organic phase, which merits its selection as a metal carrier in the present LM process. The optimization involved studies on the effects of hydrodynamic and chemical parameters such as rate of stirring, volume of LM, carrier concentration, SP acidity, and RP composition. Under the optimized conditions, Ce recovery from real and simulated waste effluents has been attempted.

EXPERIMENTAL

TBP and reagent-grade dodecane were obtained from Fluka, Germany. TBP was washed with dilute NaOH, HNO_3 ($\sim$0.5 mol·dm^{-3}), and finally with distilled water.

Radiochemically pure Ce-144 and Am-241 tracers were used. The 0.05 eluate fraction of Ce-144 and Am-241 obtained during two-step extraction chromatographic separation of HLW was also used (11). In this separation procedure the HLW solution was adjusted to 3 mol·dm^{-3} of HNO_3 concentration and passed through a chromatographic column made of CMPO adsorbed on chromosorb-102. A selective elution using 0.05 mol·dm^{-3} HNO_3 resulted in partitioning of trivalent elements from other constituents elements of HLW. This trivalent eluate fraction (mainly containing Am, Ce, Pm, Eu, etc.) was adjusted to pH 2 and again passed through the chromatographic column made up of KSM-17 adsorbed on chromosorb-102. A selective elution using 0.05 mol·dm^{-3} HNO_3 as eluant gave a trace eluate fraction of Ce–Am mixture separated from other trivalent cations. The mixture of Ce–Am thus obtained was used after adjusting its acidity to 1 mol·dm^{-3} of HNO_3. The simulated waste solutions of Ce–Am were prepared by mixing solutions with an appropriate concentration of each element. A 0.01 mol·dm^{-3} stock solution of $Ce(NO_3)_3$ was prepared by dissolving the required amount of $Ce(NO_3)_3 \cdot 6H_2O$ (E. Merck, Germany, A.R. grade) in 1 mol·dm^{-3} HNO_3. Further dilutions were made from this stock solution, and Ce-144 tracer was added to measure the ion permeability.

Procedure

LM experiments were conducted using the membrane cell shown schematically in Fig. 2. The cell compartment in which in-situ electrolysis is to be carried out was filled with 35 cm^3 feed solution (SP, a Ce^{3+} solution in HNO_3 of the desired molarity or a binary mixture of Ce–Am in 1 mol·dm^{-3} HNO_3). The strip compartment (RP) was filled with 35 cm^3 distilled water. A solution (14 cm^3) containing the desired concentration of TBP in dodecane was put at the top where it was in contact with the two aqueous solutions (SP and RP) simultaneously. The two compartments of the cell were connected through a baffle plate which restricted the intermixing of the two aqueous solutions while fast stirring was being carried out at the interfaces. In-situ electrolysis was carried out in the SP compartment by a working anode made of platinum gauze with a $\sim$20 cm^2 surface area placed in it and a platinum wire cathode dipped in 1 mol·dm^{-3} HNO_3 in the side arm of the cell. A controlled potential was applied from a dc regulated power supply unit with a direct readout for potential in volts and current in amperes. Electric motors (Heidolph, Eng-

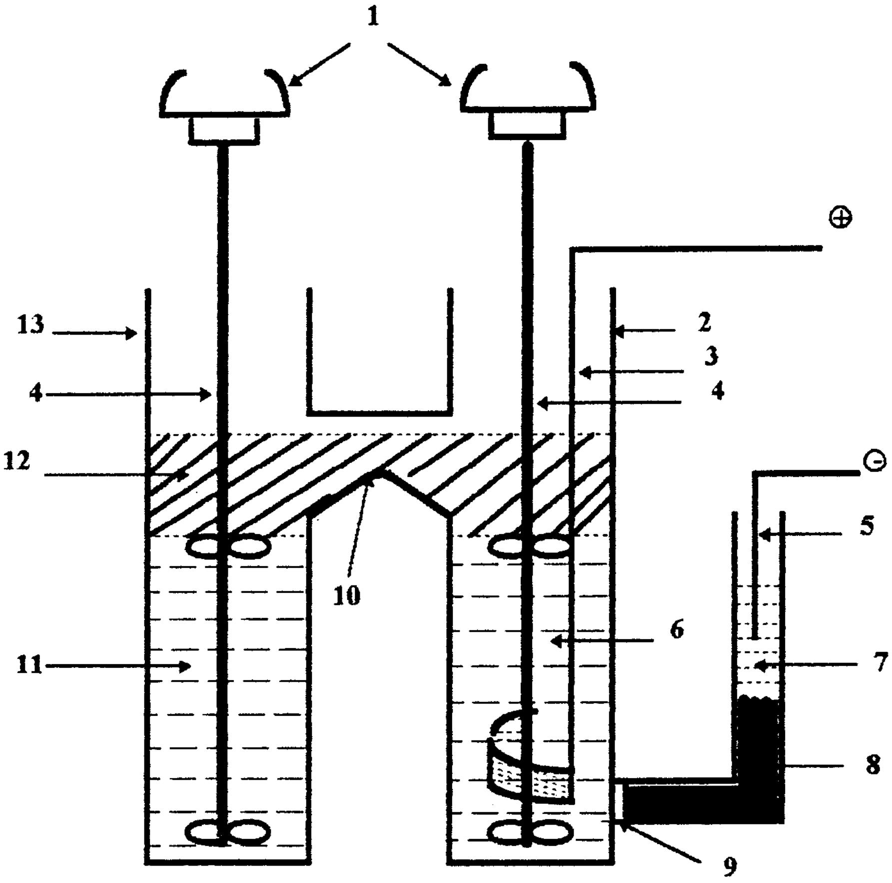

FIG. 2 Schematic diagram of liquid membrane cell. (1) Electric motors; (2) source phase compartment; (3) working gauze electrode; (4) stirring rod; (5) auxillary electrode; (6) feed solution; (7) 1 mol·dm^{-3} HNO_3, (8) agar gel; (9) fritted glass; (10) conical baffle; (11) strip solution; (12) LM phase; (13) receiving phase compartment.

land) with a speed range of 280 to 2200 rpm were used for stirring the solutions. To investigate the transport of HNO_3, the above procedure was followed by taking HNO_3 solutions of the desired concentrations containing 0.001 mol·dm^{-3} $Ce(NO_3)_3$ in the SP, distilled water in the RP, and 30% TBP/dodecane as the LM phase. The reproducibility of the permeation experiments was confirmed by repeated runs.

Sample Analysis

Suitable aliquots of the SP, RP, and LM phases were analyzed for gross alpha (2 Pi gas flow proportional counter), gross gamma ([NaI(Tl)] scintillator counter standardized against Cs-137 source), and individual gamma nuclides (62 cc HPGe detector connected to a 4K multichannel analyzer).

Permeation Measurements

The Ce^{4+} transport was determined by monitoring Ce concentrations in both the RP and SP. A molar flux of cerium, J_M, was computed using

$$J_M = d[Ce_{receiving}]/dt \cdot (V/A) \qquad mol \cdot m^{-2} \cdot s^{-1} \tag{1}$$

where $[Ce_{receiving}]$ = molar Ce concentration in RP at time t, seconds; V = volume of RP, dm^{-3}; and A = effective area of LM, m^2. Under the present experimental conditions, $V = 0.035\ dm^3$ and $A = 4.91 \times 10^{-4}\ m^2$.

RESULTS AND DISCUSSION

In comparison to normal bulk liquid membrane cells (beaker in beaker type), the single baffle plate membrane cell fabricated and used in the present work exhibits certain distinct advantages. The conical baffle plate restricts convective flux of the aqueous solutions across the LM solution even when fast stirring processes are being carried out at aqueous–organic interfaces. The interface stirring enhances the extraction and stripping efficiency in both the feed and stripping compartments, respectively. The organic phase above the apex of the cone becomes the settling zone for the LM, and this also could be stirred to reduce the concentration polarization in the LM to enhance metal transport. The amount of carrier solvent with this cell geometry is much less than that used in an integrated baffle plate cell reported by Vijayakumar et al. (20) and others (24) which requires more solvent to cover all the baffle plates. In our previous studies it was observed that whenever the organic solvent comes in direct contact with an electrode over prolonged time periods during the electrolytic oxidation of Ce^{3+} in the aqueous phase, it forms a thin coating on the electrode and makes it electrolytically passive, leading to low current efficiencies. This necessitates isolation of the electrode from the solvent extraction zone. Also, when dealing with Ce^{4+}, which is very unstable in HNO_3 medium because HNO_2 reduces it back to Ce^{3+}, fast extraction of Ce^{4+} into the organic phase is recommended (12). The cell geometry described above fulfills these conditions and extracts Ce^{4+} efficiently. The Ce complex in the continuous organic phase remains very low throughout, much lower than its equilibrium concentration. This reflects the nonequilibrium feature of the BLM process in which the extractant in the continuous organic phase shuttles back and forth between extraction and stripping compartments, acting as a "mobile carrier" to transport metal ions from feed to stripping solution continuously. Under these circumstances the extractant is never fully loaded with metal, and hence retains its metal uptake capacity throughout the experiment. The rate of transport of the metal ion across the LM is fast initially but slows down as time elapses. This trend is depicted with some representative curves

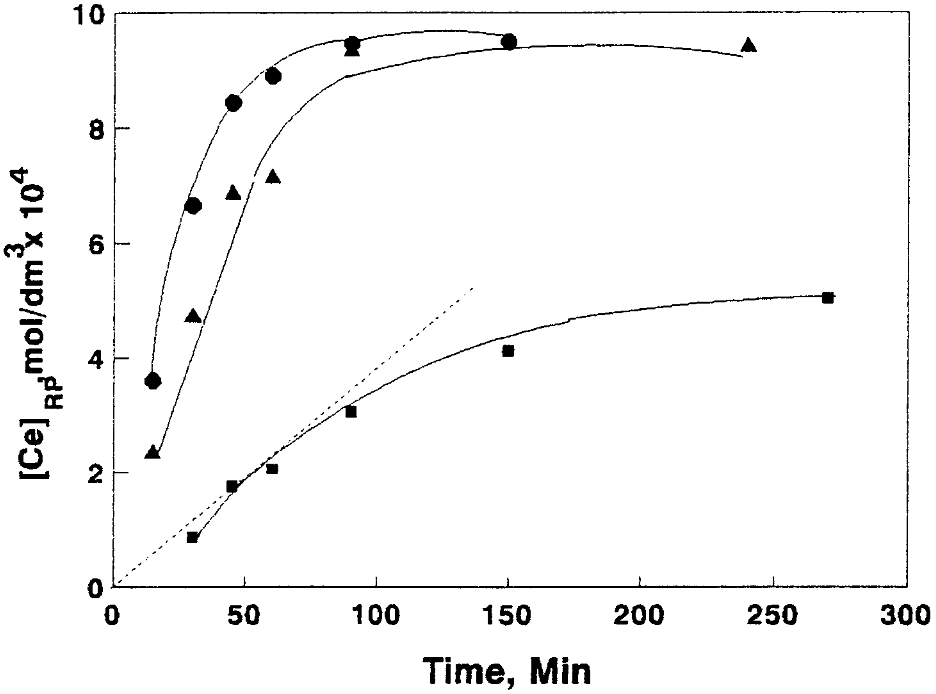

FIG. 3 Typical plot showing the variation in the concentration of Ce in the receiving phase with time: (■) 0.4 mol·dm^{-3} TBP, (▲) 1.1 mol·dm^{-3} TBP, (●) 1.5 mol·dm^{-3} TBP. Source phase = 0.001 mol·dm^{-3} $Ce(NO_3)_3$ in 1 mol·dm^{-3} HNO_3. The dotted line represents the tangent to the curve at time $t = 0$.

in Fig. 3. Similar transport kinetics were reported by Upadhyay et al. (25). This trend can be explained in terms of the postulated mechanism (17, 26, 27) of carrier-mediated transport through the LM which can be summarized as follows. The cation in the source phase is partitioned along with its anion into the membrane phase where it is complexed by the carrier ligand. The complex–anion pair moves across the membrane and is decomplexed at the membrane–receiver phase interface, releasing the cation and the anion into the receiver phase. The free carrier legand diffuses to the membrane–source phase interface and repeats the cycle. It is apparent from this mechanism that an uphill transport of metal ion from the source phase makes it deficient in metal concentration. Hence, the rate of metal ion oxidation and its diffusion in aqueous SP solution toward the membrane interface slows down, and this adds to the time taken for transport. Also, the increase of metal ions in the receiver phase increases the possibility of transport of metal ions in the reverse direction. In the present study, therefore, trends in the transport data are discussed in terms of the initial rates of transport determined by the tangent at time $t = 0$ from the curves obtained by plotting concentration of cerium in the RP against time (Fig. 3).

Effect of Stirring and Membrane Volume

The effects of hydrodynamic conditions on Ce^{4+} transport were studied at varying stirring speeds of both feed and strip phases. When the experiment is performed for 4 hours under unstirred conditions, almost negligible transport of Ce across the BLM is observed. When the feed solution alone is stirred at the bottom, comparatively much less transport of Ce is noted to that obtained when interface stirring occurs. As depicted in Fig. 2, a two-level stirring system was installed. Bottom stirring in the feed solution facilitates an upward motion of the oxidized Ce species which reduces the concentration polarization, similarly to the RP. Stirring at the interface induces a fine dispersion of aqueous drops into the organic membrane phase and hence increases the contact surface area of the two liquid phases, which in turn enhances the solvent extraction process. The optimum stirring rate is 380 and 300 rpm at the SP–LM and RP–LM interfaces, respectively. No noticeable increase in transport rate was observed above these values (Table 1). The fabricated cell geometry necessitates a minimum LM volume of 14 cm^3 with a 0.8 cm height in the settling zone. The LM volume can be increased by lowering the aqueous volume in both compartments. By increasing the LM volume while the other parameters are held constant, a gradual decrease in flux is observed. An in-

TABLE 1
Effect of Stirring Rate on the Transport of Ce^{4+} across BLM

Source phase:	0.001 $mol \cdot dm^{-3}$ $Ce(NO_3)_3$ + tracer Ce-144 in 1 $mol \cdot dm^{-3}$ of HNO_3 (35 cm^3)
Receiving phase:	Distilled water (35 cm^3)
Membrane phase:	30% TBP/dodecane (14 cm^3)
Voltage applied:	2.5 volts
Temperature:	~25°C

Stirring rate (rpm)		
SP	RP	$J_M{}^a \times 10^5$ mol/m²/s
280	280	0.54
280	340	0.82
280	360	0.97
280	380	1.22
280	400	1.40
300	380	1.44
320	380	1.43
350	380	1.44

[a] Flux of Ce^{4+} is calculated for a 5-hour transport experiment.

crease in the LM volume, which results in an increased metal complex diffusion path length inside the LM, may be the cause of the reduction of the flux rate at larger volumes of the LM.

Effect of Electrode Potential

The principle electrochemical reaction in the feed solution is (2):

$$\mathrm{Ce}^{3+} \Leftrightarrow \mathrm{Ce}^{4+} + \mathrm{e}^{-} \qquad (E_0 = +1.61\ \mathrm{V}) \tag{2}$$

The permeation experiments were performed under different applied potentials in the SP compartment. In-situ electrolysis oxidizes Ce^{3+} to extractable Ce^{4+} which transports through the BLM. There is practically no transport of Ce across the BLM recorded below 1.65 V because the standard electrode potential for Ce^{3+} to Ce^{4+} conversion in 1 $\mathrm{mol{\cdot}dm^{-3}}$ $\mathrm{HNO_3}$ is 1.61 V (28). A significant rise in flux value is obtained when the potential is increased above 1.75 V (Fig. 4). The J_M value reaches a saturation value at about 2.5 V of electrode potential. Hence, in all our experiments the applied oxidation potential was maintained at 2.5 V.

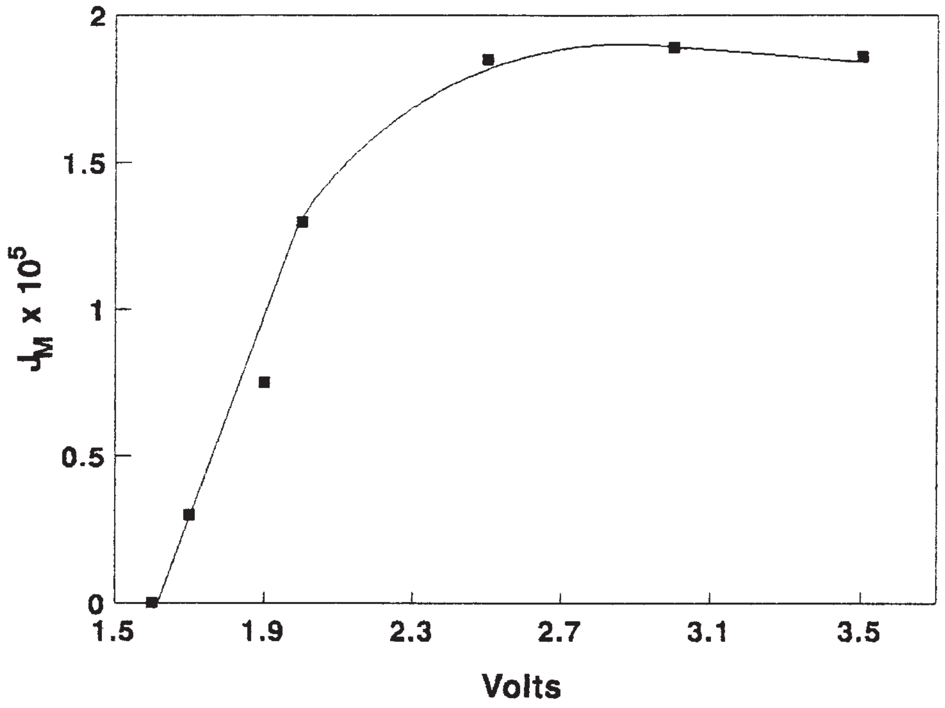

FIG. 4 Variation of J_M with applied voltage.

Effect of the Composition of Receiving Phase

Several stripping agents were used in the RP: ethylene diamine tetraacetic acid (EDTA), sodium carbonate, sodium nitrite, oxalic acid, hydrazine, hydrogen peroxide, and distilled water. Water was the best RP among those studied. When EDTA is used in the RP, a localized precipitation of EDTA in the RP at the membrane interface is observed because of the simultaneous transport of HNO_3. With dilute solutions of EDTA in the RP, no additional flux value is noted compared with that of water in the RP. A similar problem is observed with sodium carbonate where cerous carbonate precipitated because of its very low aqueous solubility. When the RP is sodium nitrite, oxalic acid, hydrazine, or hydrogen peroxide, an abrupt halt of Ce uptake by the LM in the SP compartment is observed. This may be due to the extractability and transport of these reagents in the organic LM phase from the RP to the SP, and the consequent reduction of Ce^{4+} to inextractable Ce^{3+} at the LM–SP interface.

Effect of TBP Concentration in LM

Control experiments conducted with only dodecane as the LM phase gave no transport of Ce across the BLM. This confirms the absence of convective flux across the BLM. Hence, referring to our previous solvent extraction findings (12), the following LM extraction and stripping mechanism is proposed.

$$Ce^{4+} + 4NO_3^- \Leftrightarrow Ce(NO_3)_4 \tag{3}$$

$$Ce(NO_3)_4 + 2TBP_M \Leftrightarrow Ce(NO_3)_4 \cdot 2TBP_M \tag{4}$$

$$Ce(NO_3)_4 \cdot 2TBP \text{ diffuses across the membrane} \tag{5}$$

$$Ce(NO_3)_4 \cdot 2TBP_M \Leftrightarrow Ce(NO_3)_4 + 2TBP_M \tag{6}$$

$$Ce(NO_3)_4 \Leftrightarrow Ce^{4+} + 4NO_3^- \tag{7}$$

$$Ce^{4+} + e^- \Leftrightarrow Ce^{3+} \tag{8}$$

$$\text{TBP diffuses back across the membrane} \tag{9}$$

The subscripts M indicates species in the LM.

By increasing the concentration of TBP in the BLM, a gradual increase in transport of Ce was observed. A plot of log J_M vs log[TBP] in the BLM is given in Fig. 5 [experimental conditions: SP phase = 1 mol·dm^{-3} HNO_3 containing 0.001 mol·dm^{-3} $Ce(NO_3)_3$, RP phase = distilled water, LM phase = mixtures of TBP–dodecane]. The solubility of TBP in the aqueous phase was

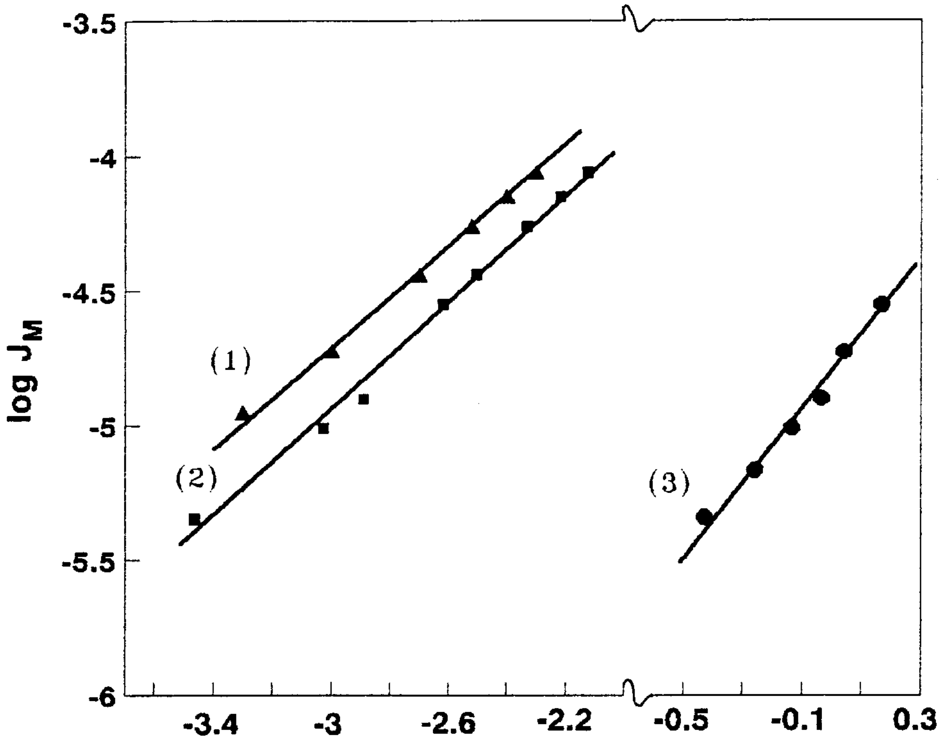

FIG. 5 Plot of log J_M against (1) log[Ce^{3+}], (2) 1.34 log[TBP] + log[Ce^{3+}], (3) log[TBP].

very much less under the given experimental conditions (<0.1 g/dm^3) and hence was considered negligible in our further calculations. The concentrations of free TBP in the BLM were calculated as the difference between the actual TBP taken and the TBP complexed with HNO_3. The concentrations of the TBP–HNO_3 complex were determined by monitoring the acidity of the BLM phase. A straight line with a slope $a = 1.34$ is obtained, which is less than the expected value of 2, represented by Eq. (4). An increase in the concentration of TBP enhances the reaction shown in Eq. (4) in the forward direction, but this condition is not favorable to the reactions given in Eqs. (5) and (6). Equation (5) is mainly controlled by the viscosity of the BLM phase. An increase in the concentration of TBP in dodecane also increases the viscosity of the solution, which generates more resistance to diffusion of the Ce–TBP complex across the LM phase. Similarly, increasing the concentration of TBP in the LM phase reduces the forward thrust of the reaction given in Eq. (6). Hence, increasing the concentration of TBP in the LM phase favors Eq. (4) but adversely affects the reactions represented by Eqs. (5) and (6). Also, for diluent–TBP interactions, only molar concentrations of TBP are used instead of its actual activity values. All these might have contributed to the deviation of the a value.

Effect of HNO_3 Concentration in SP

Table 2 shows the dependence of J_M on the source phase HNO_3 concentration. With an increase in HNO_3 concentration in the SP, the average flux of Ce increases and reaches saturation at around 4 mol·dm^{-3} of HNO_3. Even though

TABLE 2
Transport of Ce^{4+} across BLM as a Function of Nitric Acid Concentration in the Source Phase

Source phase:	0.001 mol·dm^{-3} $Ce(NO_3)_3$ + tracer Ce-144 (35 cm^3)
Receiving phase:	Distilled water (35 cm^3)
Membrane phase:	30% TBP/dodecane (14 cm^3)
Voltage applied:	2.5 volts
Temperature:	~25°C

[HNO_3] (mol·dm^{-3})	Time (min)	$J_M \times 10^5$ mol/m^2/s	Permeation (%)
0.5	15	0.32	4.1
	30	0.25	6.3
	45	0.18	6.8
	60	0.16	8.1
	180	0.14	21.3
1.0	15	1.88	23.8
	30	1.88	47.6
	45	1.82	68.9
	60	1.44	71.7
	180	0.62	94.5
2.5	15	2.35	29.7
	30	2.10	53.0
	45	2.05	77.6
	60	1.75	88.3
	180	0.60	91.3
3.5	15	2.64	33.4
	30	2.20	55.5
	45	1.72	65.1
	60	1.55	78.5
	180	0.59	90.1
4.2	15	2.73	34.5
	30	2.35	59.5
	45	1.78	67.3
	60	1.57	79.4
	180	0.57	85.8
5.1	15	1.79	22.6
	30	1.51	38.2
	45	1.39	52.7
	60	1.29	65.3
	180	0.49	74.5

the flux value for Ce at 4 mol·dm^{-3} is maximum, the permeation yield of Ce in the RP after 3 hours was maximum at 1 mol·dm^{-3} of HNO_3 in the SP. The extractive permeation of Ce across the BLM is predominantly governed by Eqs. (3) and (4). The initial increase in J_M with respect to the increase in the SP HNO_3 concentration is due to the salting out effect of increasing NO_3 concentration. TBP also forms a complex with HNO_3, and hence cotransport of HNO_3 across the BLM was noted (Fig. 6). The transport of HNO_3 is governed by the following reaction:

$$H^+ + NO_3^- + TBP_M \Leftrightarrow HNO_3{\cdot}TBP_M \tag{10}$$

The transport of HNO_3 across the BLM was studied by taking different concentrations of HNO_3 in the SP. The flux of HNO_3 across the BLM increases with increasing concentration of HNO_3 in the SP. As shown in Fig. 6, Eq. 10 becomes more predominant at higher nitric acid concentrations and more transport of HNO_3 across the BLM occurs. This also hinders any further rise in Ce transport with increasing HNO_3 concentration in the SP. An increase in HNO_2 concentration in the SP at higher nitric acid concentrations may also reduce the yield of Ce^{4+}. In the presence of $NO_2{}^-$, Ce^{4+} reduces back to Ce^{3+},

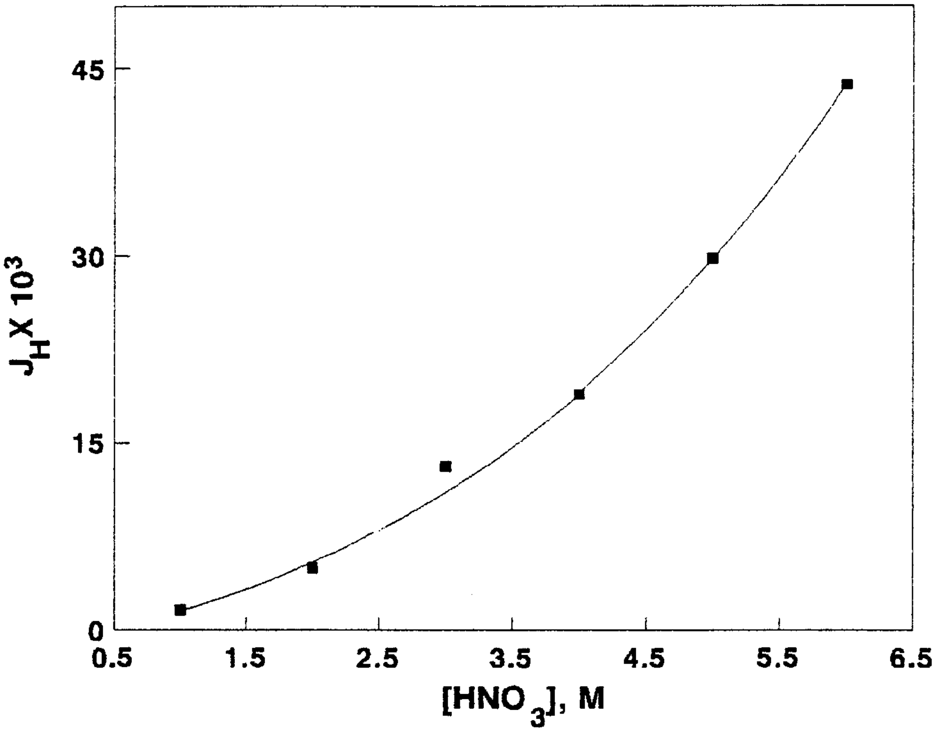

FIG. 6 Flux of HNO_3 with increasing [HNO_3] in the source phase. LM = 1.1 mol·dm^{-3} TBP/dodecane, SP = 0.001 mol·dm^{-3} $Ce(NO_3)_3$ in HNO_3, RP = distilled water.

which is a fast reaction. This may be the reason for the lowering of J_M values above 4 mol·dm^{-3} of HNO_3 in the SP.

Effect of Ce Concentration

The flux of Ce^{4+} across the BLM was found to be a function of the metal salt concentration in the source phase. As Ce^{3+} has negligible extraction in 30% TBP/dodecane, all the Ce present in the organic phase was assumed to be Ce^{4+} and which has limited stability in the organic phase because it reverts to Ce^{3+} and is stripped from the organic phase. Hence, the overall transport of Ce is influenced by the initial concentration of Ce^{3+} in the aqueous phase and the efficiency of the electrooxidation process applied. The precise concentration of Ce^{4+} is difficult to calculate under these transient conditions although it could have given more meaningful information. The plot of log J_M against log $[Ce^{3+}]$ is a straight line (Fig. 5) under the experimental conditions of SP phase = 1 mol·dm^{-3} HNO_3, LM phase = 30% TBP/dodecane, and RP phase = distilled water. The slope of the straight line plot obtained is 1. Such linearity has been reported by several authors (17, 25, 29). On the basis of the linear relation obtained between molar flux and the concentration of TBP in the LM phase, as well as the initial concentration of Ce^{3+} in the SP, an equation for the molar flux (J_M) of Ce^{4+} can be derived as shown in Eq. (11). The other experimental conditions for this correlation are SP phase = 1 mol·dm^{-3} HNO_3 (35 cm^3), RP phase = distilled water (35 cm^3), LM phase = TBP/dodecane (14 cm^3), and optimum stirring conditions at room temperature (~ 25°C).

$$J_M = K\,[\text{TBP}]^a[Ce^{3+}]^b \qquad \text{mol·m}^{-2}\text{·s}^{-1} \tag{11}$$

where K is a molar flux constant and the values for the exponents a and b were determined experimentally to be 1.34 and 1, respectively, from the slope of their log–log correlation. To obtain the value for the molar flux constant K, log J_M is plotted against log $([\text{TBP}]^{1.34}[Ce^{3+}])$ as shown in Fig. 5. The slope of the line is approximately 1 and the intercept point is -2.1, which gives $K = 7.94 \times 10^{-3}$.

Selective Transport of Ce from Ce-Am Mixture

Transport experiments were carried out when feed solutions were Ce-Am mixtures obtained from extraction chromatographic partitioning of high level radioactive waste solutions (11). As shown by the data presented in Table 3, there is no effect of the presence of Am in the SP on the flux of Ce across the BLM. The gamma spectrums of the initial SP, the SP after 5 hours of the transport experiment, the RP after 5 hours of transport, and the LM after 5 hours were recorded. The feed solution was a fraction of Ce–Am obtained from the

TABLE 3
Permeation of Ce^{4+} across BLM from Simulated Waste Solutions

Source phase: 1 $mol \cdot dm^{-3}$ HNO_3 + Ce (35 cm^3)
Receiving phase: Distilled water (35 cm^3)
Membrane phase: 30% TBP/dodecane (14 cm^3)
Voltage applied: 2.5 volts
Temperature: ~25°C

Origin of waste solution[a]	Initial [Ce] in SP (mg/dm^3)	Initial [Am] in SP[b] (mg/dm^3)	[Ce] in RP after 5 h (mg/dm^3)	[Am] in SP after 5 h (mg/dm^3)	Maximum[c] $J_M \times 10^5$ $mol/m^2/s$ Exp	Cal	Permeability[d] of Ce (%)
HWR/HLW	0.6	0.52	0.54	0.52	0.006	0.007	90.6
PHWR/HLW	532.5	0.49	497	0.50	3.98	4.58	93.4
FBR/HLW	684.1	0.52	633	0.51	5.22	5.81	92.6

[a] A mixture of Ce–Am was prepared by taking the corresponding Ce concentration as reported by Mathur et al. (30) in the waste solutions (Heavy Water Reactor, HWR-HLW; Pressurised Heavy Water Reactor, PHWR-HLW; and Fast Breeder Reactor, FBR-HLW).

[b] Am concentration was maintained ca. 0.5 mg/dm^3.

[c] Maximum J_M is calculated by drawing a tangent at time = 0 to the curves [Ce] in the receiving phase vs time.

[d] Permeability is calculated for 5-hour transport experiments.

actual HLW solution. The gamma spectrum of the SP after 5 hours shows an almost quantitative retention of Am (peak at 60 keV) while more than a 90% reduction of the peak height at 133 keV due to Ce-144 is seen. The receiving phase predominantly shows gamma activity due to Ce-144 and practically no gamma activity in the vicinity of 60 keV, and hence complete elimination of Am in the product solution. This was also confirmed by alpha counting of the RP where no detectable alpha activity due to Am was observed. To cover the whole range of waste solution compositions as described by Mathur et al. (30), simulated solutions with different Ce–Am concentrations were prepared and from these the transport of Ce across the BLM was investigated (Table 3). For analytical simplicity a fixed amount of Am-241 was taken in all these studies. The removal of Ce from the feed solution resulted in purification of Am with respect to Ce activity and the decontamination factor is of the order of 12.

CONCLUSION

Transport of Ce^{4+} ion through a BLM containing TBP as a carrier has been studied under different hydrodynamic and chemical conditions. The single baffle plate BLM cell used in the experiment is highly efficient and very simple to operate. The flux for cerium is found to depend on the concentrations of TBP, cerous salt, nitric acid, and the applied oxidation potentials. An equation for the permeation velocity of the Ce^{4+} ion is proposed under the specified experimental conditions. The separation and reduction of Ce in a Ce–Am mixture obtained from extraction chromatographic separation facilitates the subsequent handling of Am for partitioning and transmutation studies. The present approach gives a satisfactory partitioning of Ce from a Ce–Am mixture in nitric acid medium. The technique can also be used for the separation of different cationic mixtures.

ACKNOWLEDGMENTS

The authors thank Shri. K. Balu, Director, FR & NWM Group, and Shri. V. P. Kansara, Head, FRD, for their keen interest in this work. They also thank Dr. P. V. Achuthan for the fruitful discussions carried out during the preparation of this manuscript.

REFERENCES

1. K. L. Nash, *Sol. Extr. Ion Exch., 11*, 729 (1993).
2. K. A. Gschneider (Ed.), *Industrial Applications of Rare Earth Elements* (ACS Symp. Ser. 164), American Chemical Society, Washington, DC, 1981.
3. S. Tani, M. Ozawa, and T. Wakabayashi, *Proceedings of the IAEA Technical Committee Meeting on Safety and Environmental Aspects of Partitioning and Transmutation Actinides and Fission Products. Vienna, November 29–December 2*, 1993.
4. L. H. Baetsle., *Atomtech, 38*, 226 (1993).
5. Z. Kolarik, *Report Kfk 4945* (1991).
6. T. D. Filer, *Anal. Chem., 46*, 608 (1974).
7. J. D. Navratil and W. W. Schulz (Eds.), *Transplutonium Elements: Production and Recovery* (ACS Symp. Ser. 16), American Chemical Society, Washington, DC, 1981.
8. G. R. Choppin, J. D. Navratil, and W. W. Schultz, (Eds), *Acitinide/Lanthanide Separations*, World Scientific, Singapore, 1985.
9. I. L. Jenkins, *Solv. Extr. Ion Exch., 2*, 1 (1984).
10. J. N. Mathur, M. S. Murali, P. R. Natarajan, L. P. Badheka, A. Banerji, A. Ramanujam, P. S. Dhami, V. Gopalkrishnan, R. K. Dhumwad, and M. K. Rao, *Waste Manage., 13*, 317 (1993).
11. A. Ramanujam, P. V. Achuthan, P. S. Dhami, V. Gopalkrishnan, R. Kannan, and J. N. Mathur, *Solv. Extr. Ion Exch., 13*, 301 (1995).
12. C. S. Kedari, S. S. Pandit, and A. Ramanujam, *J. Radioanal. Nucl. Chem., 222*, 141 (1997).
13. T. C. Huang and R. S. Juang, *J. Membr. Sci., 31*, 209 (1987).
14. S. G. Nair and S. T. Hwang, *Ibid., 64*, 69 (1991).
15. R. Mohapatra and S. B. Kanungo, *Sep. Sci. Technol., 27*, 1759 (1992).
16. A. M. Urtiaga, M. I. Ortiz, and E. Salazar, *Ind. Eng. Chem. Res., 31*, 877 (1992).
17. J. D. Lamb, J. J. Christensen, S. R. Izatt, K. Bedke, M. S. Astin, and R. M. Izatt, *J. Am. Chem. Soc., 102*, 3399 (1980).

18. P. R. Danesi, *Sep. Sci. Technol.*, *19*, 857 (1984).
19. W. S. W. Ho and K. K. Sirkar (Eds.), *Membrane Hand Book*, Van Nostrand Reinhold, New York, NY, 1992.
20. S. Vijayakumar, M. Ravindram, M. Chandra, and J. R. Mudakavi, *Indian J. Chem. Technol.*, *1*, 131 (1994).
21. W. W. Schultz and J. D. Navaratil (Eds.), *Science and Technology of Tributyl Phosphate Vols. 1–3*, CRC Press, Boca Raton, FL, 1984.
22. J. P. Shukla and S. K. Misra, *J. Membr. Sci.*, *64*, 93 (1991).
23. M. Chaudry, Noor-Ul-Islam, and D. Mohammad, *J. Radioanal. Nucl. Chem.*, *109*, 11 (1987).
24. Z.-M. Gu, *J. Membr. Sci.*, *52*, 77 (1990).
25. S. Upadhyay, V. A. Varghese, L. Mishra, S. N. Singh, and R. C. Srivastava, *Ibid.*, *93*, 149 (1994).
26. W. J. Ward, *AIChE J.*, *16*, 405 (1970).
27. C. F. Reusch and E. L. Cussler, *Ibid.*, *19*, 736 (1973).
28. J. J. Lingane, (Ed.), *Electro analytical Chemistry*, Interscience, New York, NY, 1958.
29. T. Saito, *Sep. Sci. Technol.*, *25*, 581 (1990).
30. J. N. Mathur, M. S. Murali, M. V. Balaramakrishna, R. H. Iyer, R. R. Chitnis, P. K. Wattal, T. K. Theyyunni, A. Ramanujam, P. S. Dhami, and V. Gopalkrishnan, *Ibid.*, *31*, 2045 (1996).

Received by editor January 5, 1998
Revision received June 1998

Marcel Dekker, Inc.
270 Madison Avenue, New York, New York 10016

PAGE 1924 IS BLANK

MARCEL DEKKER, INC.
270 Madison Avenue, New York, New York 10016

Downloaded At: 11:09 25 January 2011

Request Permission or Order Reprints Instantly!

Interested in copying and sharing this article? In most cases, U.S. Copyright Law requires that you get permission from the article's rightsholder before using copyrighted content.

All information and materials found in this article, including but not limited to text, trademarks, patents, logos, graphics and images (the "Materials"), are the copyrighted works and other forms of intellectual property of Marcel Dekker, Inc., or its licensors. All rights not expressly granted are reserved.

Get permission to lawfully reproduce and distribute the Materials or order reprints quickly and painlessly. Simply click on the "Request Permission/Reprints Here" link below and follow the instructions. Visit the U.S. Copyright Office for information on Fair Use limitations of U.S. copyright law. Please refer to The Association of American Publishers' (AAP) website for guidelines on Fair Use in the Classroom.

The Materials are for your personal use only and cannot be reformatted, reposted, resold or distributed by electronic means or otherwise without permission from Marcel Dekker, Inc. Marcel Dekker, Inc. grants you the limited right to display the Materials only on your personal computer or personal wireless device, and to copy and download single copies of such Materials provided that any copyright, trademark or other notice appearing on such Materials is also retained by, displayed, copied or downloaded as part of the Materials and is not removed or obscured, and provided you do not edit, modify, alter or enhance the Materials. Please refer to our Website User Agreement for more details.

Order now!

Reprints of this article can also be ordered at

http://www.dekker.com/servlet/product/DOI/101081SS100100746